Proton and neutron electromagnetic radii and magnetic moments from lattice QCD

Miguel Salg, Dalibor Djukanovic, Georg von Hippel, Harvey B. Meyer, Konstantin Ottnad, Hartmut Wittig

[arXiv:2309.06590], [arXiv:2309.07491], [arXiv:2309.17232]

MENU 2023, October 16, 2023

Outline

Outline

Motivation

- "Proton radius puzzle": discrepancy between different determinations of the electric and magnetic radii of the proton
- In lattice QCD as in the context of scattering experiments: radii extracted from electromagnetic form factors
- Tension between Q^2-dependence of form factors from different experiments

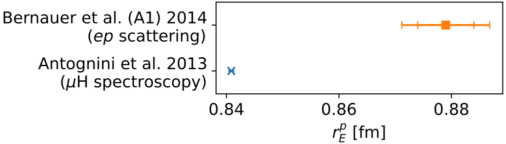

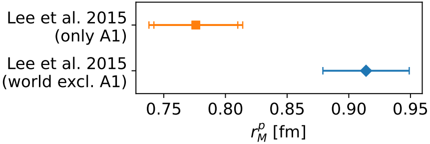

- Full calculation of the proton and neutron form factors from first principles necessitates explicit treatment of the numerically challenging quark-disconnected contributions
- Neglected in many previous lattice studies, in particular no simultaneous control of all relevant systematics

Outline

QCD on the lattice

- Coupling of QCD is large at large distances / low energies
- Low-energy regime of QCD is hence inaccessible to perturbative methods
- Powerful tool for the non-perturbative study: lattice QCD
- Replace space-time by a four-dimensional Euclidean lattice
- Gauge-invariant UV-regulator for the quantum field theory due to the momentum cut-off
- Path integral becomes finite-dimensional and can be computed numerically
- Allows a systematic extrapolation to the continuum and infinite-volume limit, $a \to 0$ and $V \to \infty$

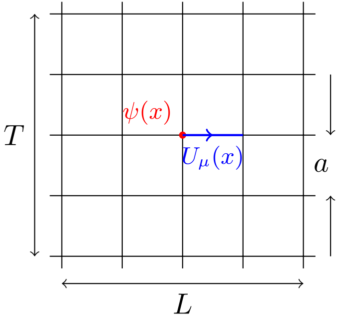

Ensembles

Coordinated Lattice Simulations (CLS)[1]

- Non-perturbatively $\mathcal{O}(a)$-improved Wilson fermions
- $N_f = 2 + 1$: 2 degenerate light quarks ($m_u = m_d$), 1 heavier strange quark ($m_s > m_{u,d}$)
- $\mathrm{tr}\, M_q = 2m_l + m_s =$ const.
- Tree-level improved Lüscher-Weisz gauge action
- $\mathcal{O}(a)$-improved conserved vector current

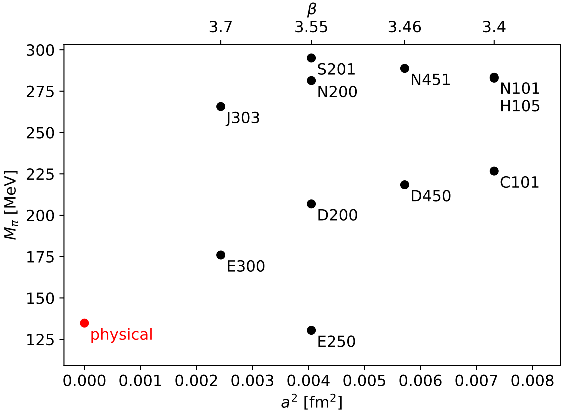

Figure: Overview of the ensembles used in this study

[1] Bruno et al. 2015 [JHEP **2015** (2), 43]; Bruno, Korzec, and Schaefer 2017 [PRD **95**, 074504].

Nucleon two- and three-point correlation functions

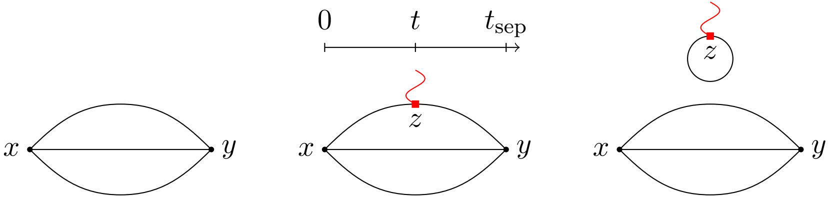

C_2 $\quad C_3^{\mathrm{conn}}$ $\quad C_3^{\mathrm{disc}}$

- Measure the two- and three-point correlation functions of the nucleon
- For three-point functions, Wick contractions yield connected and disconnected contribution
- Compute the quark loops via a stochastic estimation using a frequency-splitting technique[2]
- Extract the effective form factors $G_{E,M}^{\mathrm{eff}}$ using the ratio method[3]

[2] Giusti et al. 2019 [EPJC **79**, 586]; Cè et al. 2022 [JHEP **2022** (8), 220]; [3] Korzec et al. 2009 [PoS **066**, 139].

Excited-state analysis

- Cannot construct exact interpolating operator for the proton (any hadron) on the lattice
- All possible states with the same quantum numbers contribute
- Effect of heavier excited states suppressed exponentially with the distance between operators in Euclidean time
- For baryons, the relative statistical noise grows also exponentially with the source-sink separation $t_{\mathrm{sep}} = y_0 - x_0$

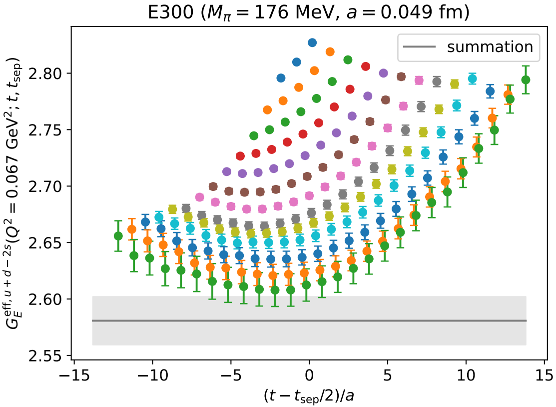

Excited-state analysis: summation method

- Explicit treatment of the excited-state systematics required
- Summation of the effective form factors over the operator insertion time,

$$S_{E,M}(Q^2; t_{\mathrm{sep}}) = \sum_{t=t_{\mathrm{skip}}}^{t_{\mathrm{sep}}-t_{\mathrm{skip}}} G^{\mathrm{eff}}_{E,M}(Q^2; t, t_{\mathrm{sep}}), \quad t_{\mathrm{skip}} = 2a \tag{1}$$

- Parametrically suppresses the effects of excited states ($\propto e^{-\Delta t_{\mathrm{sep}}}$ instead of $\propto e^{-\Delta t}$, $e^{-\Delta(t_{\mathrm{sep}}-t)}$ [Δ: energy gap to lowest-lying excited state]) $\to$ "summation method"
- For $t_{\mathrm{sep}} \to \infty$, the slope as a function of t_{sep} is given by the ground-state form factor,

$$S_{E,M}(Q^2; t_{\mathrm{sep}}) \xrightarrow{t_{\mathrm{sep}}\to\infty} C_{E,M}(Q^2) + \frac{1}{a}(t_{\mathrm{sep}} + a - 2t_{\mathrm{skip}}) G_{E,M}(Q^2) \tag{2}$$

Excited-state analysis: window average

- Apply summation method with varying starting values $t_{\mathrm{sep}}^{\mathrm{min}}$ for the linear fit
- Perform a weighted average over $t_{\mathrm{sep}}^{\mathrm{min}}$, where the weights are given by a smooth window function[4]

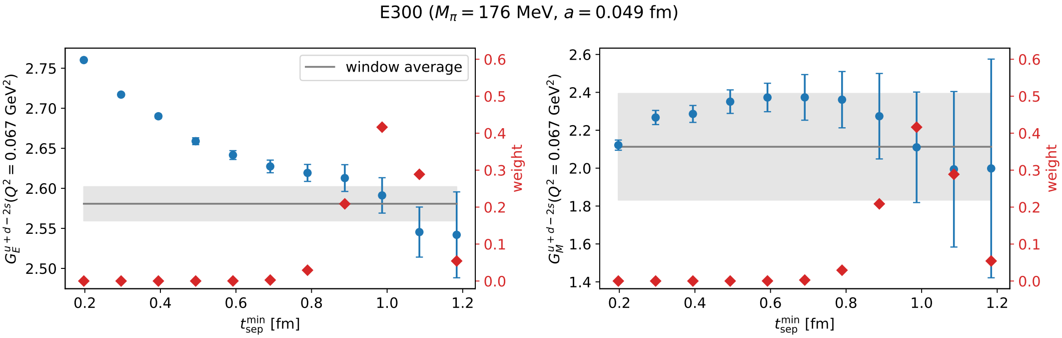

[4]Djukanovic et al. 2022 [PRD **106**, 074503]; Agadjanov et al. 2023 [arXiv:2303.08741].

Excited-state analysis: window average

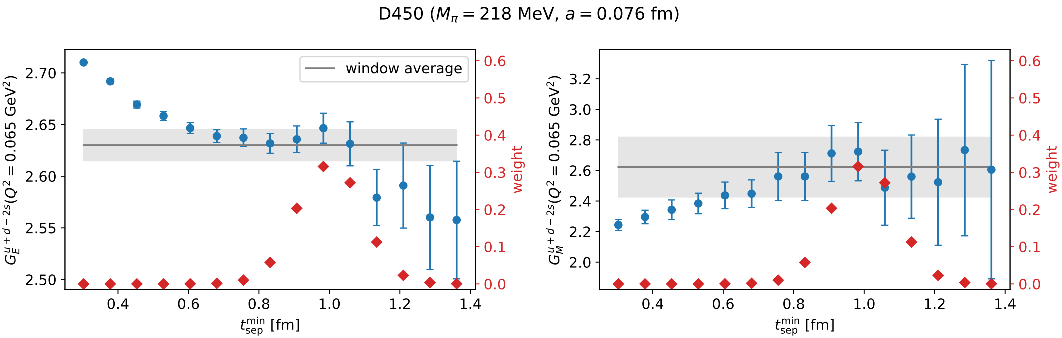

- Reliable detection of the plateau with reduced human bias (same window on all ensembles)
- Conservative error estimate

Outline

Direct Baryon χPT fits

- Combine parametrization of the Q^2-dependence with the chiral, continuum, and infinite-volume extrapolation
- Simultaneous fit of the pion-mass, Q^2-, lattice-spacing, and finite-volume dependence of the form factors to the expressions resulting from covariant chiral perturbation theory[5]
- Include contributions from the ρ (ω and ϕ) mesons in the isovector (isoscalar) channel
- Reconstruct proton and neutron observables from separate fits to the isovector and isoscalar form factors
- Perform fits with various cuts in M_π and Q^2, as well as with different models for the lattice-spacing and finite-volume dependence, in order to estimate systematic uncertainties
- Large number of degrees of freedom $\Rightarrow$ improved stability against lowering the Q^2-cut

[5] Bauer, Bernauer, and Scherer 2012 [PRC **86**, 065206].

Q^2-dependence of the isovector form factors on E300

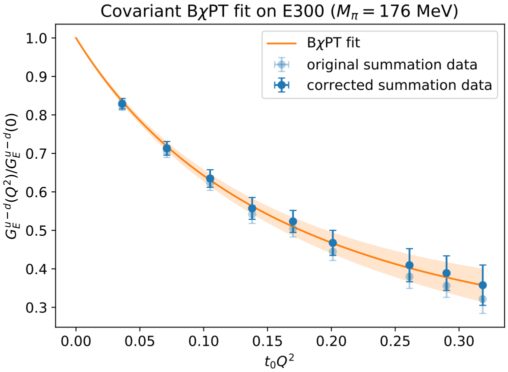

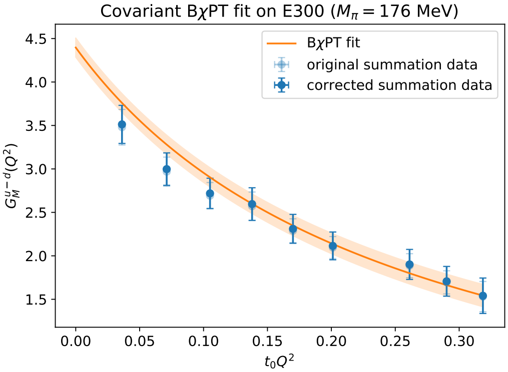

- Direct BχPT fit describes data very well
- Reduced error due to the inclusion of several ensembles in one fit

Q^2-dependence of the isoscalar form factors on E300

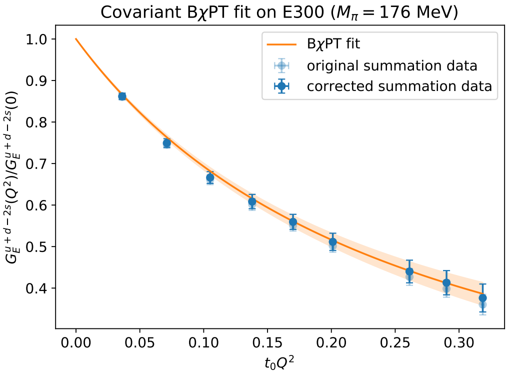

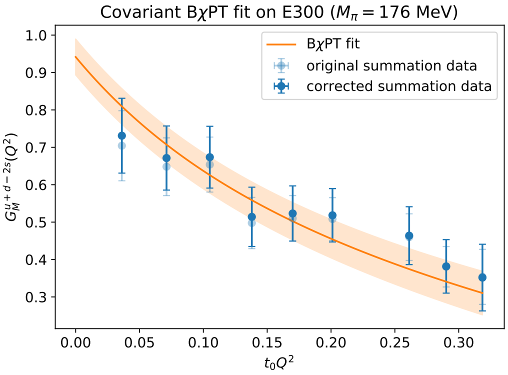

Outline

Model average

- Perform a weighted average over the results of all fit variations, using weights derived from the Akaike Information Criterion[6],

$$w_i = \exp\left(-\frac{1}{2}\mathrm{BAIC}_i\right) \Bigg/ \sum_j \exp\left(-\frac{1}{2}\mathrm{BAIC}_j\right)\,, \quad \mathrm{BAIC}_i = \chi^2_{\mathrm{noaug,min},i} + 2n_{f,i} + 2n_{c,i}, \tag{3}$$

  where n_f is the number of fit parameters and n_c the number of cut data points
- Strongly prefers fits with low n_c, *i.e.*, the least stringent cut in Q^2 $\Rightarrow$ apply a flat weight over the different Q^2-cuts to ensure strong influence of our low-momentum data
- Determine the final cumulative distribution function (CDF) from the weighted sum of the bootstrap distributions[7]
- Quote median of this CDF together with the central $68\,\%$ percentiles

[6] Akaike 1974 [IEEE Trans. Autom. Contr. **19**, 716]; Neil and Sitison 2022 [arXiv:2208.14983]; [7] Borsányi et al. 2021 [Nature **593**, 51].

CDFs of the electromagnetic radii and magnetic moment of the proton

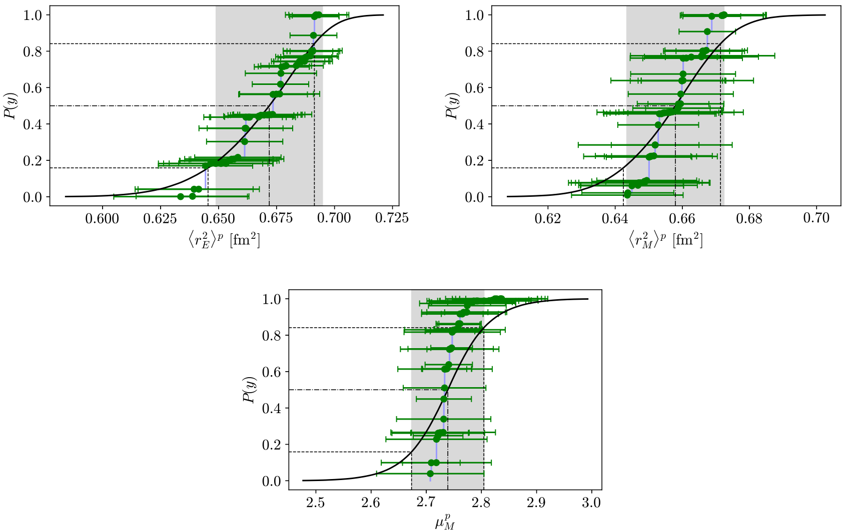

Model-averaged proton form factors at the physical point

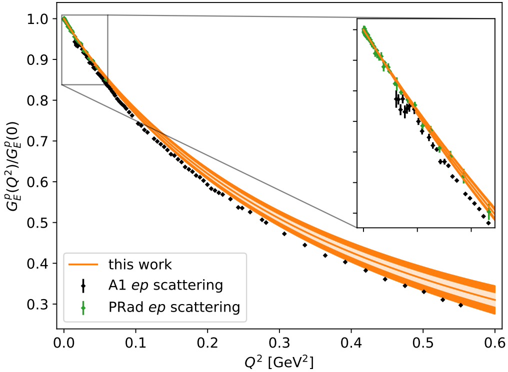

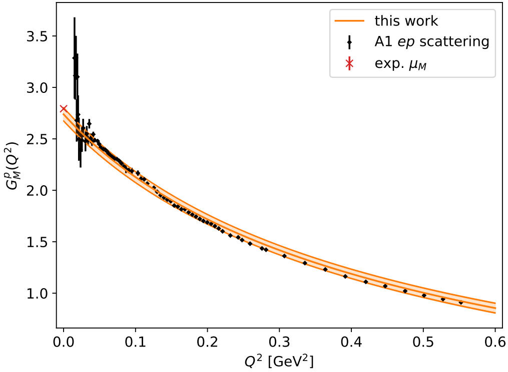

- Slope of the electric form factor closer to that of PRad[8] than to that of A1[9]
- Good agreement with A1 for the magnetic form factor

[8] Xiong et al. 2019 [Nature **575**, 147]; [9] Bernauer et al. 2014 [PRC **90**, 015206].

Model-averaged neutron form factors at the physical point

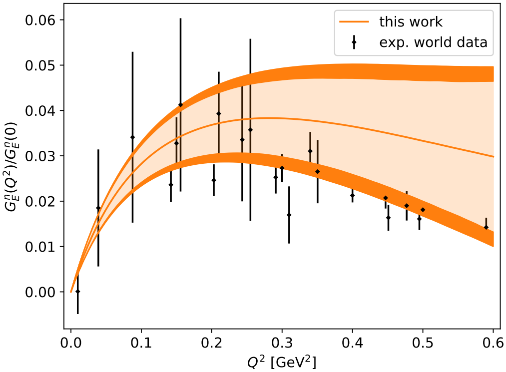

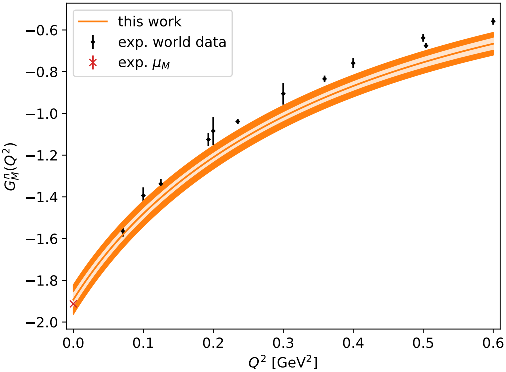

(Mostly) compatible with the collected experimental world data[10] within our errors

[10] Ye et al. 2018 [PLB **777**, 8].

Electromagnetic radii and magnetic moments

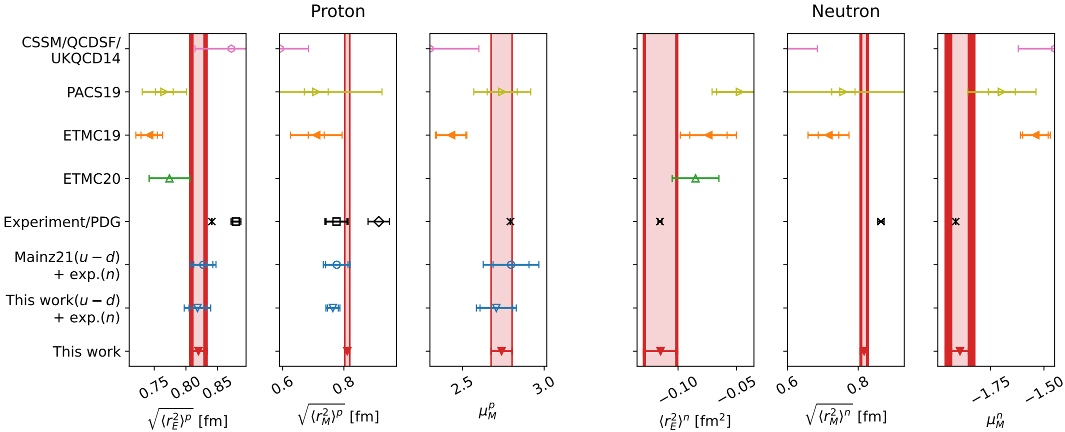

Magnetic moments reproduced, low value for $\sqrt{\langle r_E^2\rangle^p}$ clearly favored, $\sqrt{\langle r_M^2\rangle^p}$ agrees with A1

Outline

Hyperfine splitting and the Zemach radius

- Determination of nuclear properties from atomic physics
- Magnetic spin-spin interaction between the nucleus and the orbiting lepton gives rise to the hyperfine splitting (HFS)
- Electromagnetic structure of the proton influences the HFS of the S-state of hydrogen
- Relevant parameter deduced from the HFS: Zemach radius[11],

$$r_Z^p = -\frac{4}{\pi}\int_0^\infty \frac{dQ}{Q^2}\left(\frac{G_E^p(Q^2)G_M^p(Q^2)}{\mu_M^p} - 1\right) = -\frac{2}{\pi}\int_0^\infty \frac{dQ^2}{(Q^2)^{3/2}}\left(\frac{G_E^p(Q^2)G_M^p(Q^2)}{\mu_M^p} - 1\right) \tag{4}$$

- Firm theoretical prediction of the Zemach radius required both to guide the atomic spectroscopy experiments and for the interpretation of their results

[11] Zemach 1956 [Phys. Rev. **104**, 1771]; Pachucki 1996 [PRA **53**, 2092].

Zemach radius from the lattice

- BχPT including vector mesons only trustworthy for $Q^2 \lesssim 0.6\,\mathrm{GeV}^2$
- Tail of the integrand suppressed: contribution of the form factors above $0.6\,\mathrm{GeV}^2$ to r_Z less than $0.9\,\%$
- Extrapolate BχPT fit results using a z-expansion[12] *ansatz*
- Incorporate the large-Q^2 constraints on the form factors[13]
- For integration, smoothly replace BχPT parametrization by z-exp.

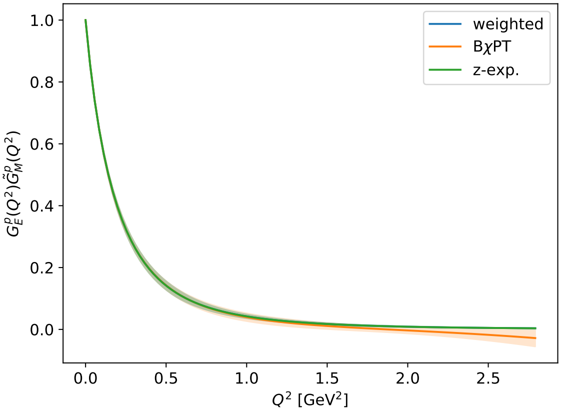

[12] Hill and Paz 2010 [PRD **82**, 113005]; [13] Lepage and Brodsky 1980 [PRD **22**, 2157]; Lee, Arrington, and Hill 2015 [PRD **92**, 013013].

Comparison to other studies

- Model-averaged result:
  $r_Z^p = 1.013(15)$ fm
  $\Rightarrow$ low value favored
- Agrees within $2\,\sigma$ with most of the experimental determinations
- Our estimate is $\sim 80\,\%$ correlated with the electromagnetic radii (based on the same form factor data)
- Low result for r_Z^p expected, no independent puzzle

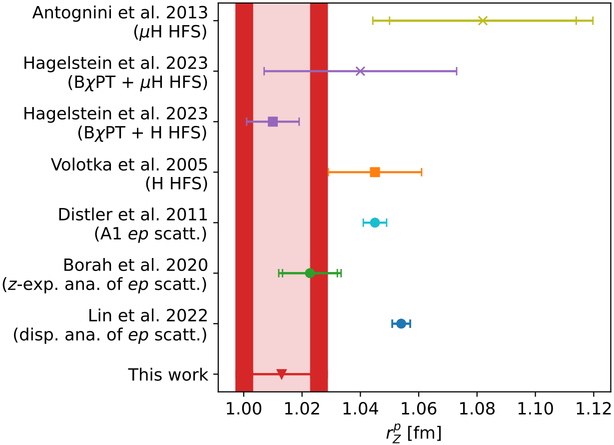

Outline

Conclusions

- Determination of the electromagnetic form factors of the proton and neutron from lattice QCD including connected and disconnected contributions, as well as a full error budget
- Chiral, continuum, and infinite volume extrapolation via matching with the predictions from covariant baryon chiral perturbation theory
- Magnetic moments of the proton and neutron agree well with the experimental values
- Small electric *and* magnetic radii of the proton favored
- Competitive errors, in particular for the magnetic radii
- First lattice calculation of the Zemach radius of the proton $\rightarrow$ small value favored ($80\,\%$ correlation with electromagnetic radii)
- Further investigations required, in particular for the magnetic proton radius

Backup slides

From correlation functions to form factors

- Average over the forward- and backward-propagating nucleon and over x-, y-, and z-polarization for the disconnected part
- Calculate the ratios

$$R_{V_\mu}(\mathbf{q};t_{\text{sep}},t) = \frac{C_{3,V_\mu}(\mathbf{q};t_{\text{sep}},t)}{C_2(\mathbf{0};t_{\text{sep}})}\sqrt{\frac{\bar{C}_2(\mathfrak{q};t_{\text{sep}}-t)C_2(\mathbf{0};t)C_2(\mathbf{0};t_{\text{sep}})}{C_2(\mathbf{0};t_{\text{sep}}-t)\bar{C}_2(\mathfrak{q};t)\bar{C}_2(\mathfrak{q};t_{\text{sep}})}}, \tag{5}$$

where $t_{\text{sep}} = y_0 - x_0$, $t = z_0 - x_0$, and $\bar{C}_2(\mathfrak{q};t_{\text{sep}}) = \sum_{\tilde{\mathbf{q}}\in\mathfrak{q}} C_2(\tilde{\mathbf{q}};t_{\text{sep}}) \Big/ \sum_{\tilde{\mathbf{q}}\in\mathfrak{q}} 1$

- At zero sink momentum, the effective form factors can be computed from the ratios as

$$G_E^{\text{eff}}(Q^2;t_{\text{sep}},t) = \sqrt{\frac{2E_{\mathbf{q}}}{m+E_{\mathbf{q}}}}R_{V_0}(\mathbf{q};t_{\text{sep}},t), \tag{6}$$

$$G_M^{\text{eff}}(Q^2;t_{\text{sep}},t) = \sqrt{2E_{\mathbf{q}}(m+E_{\mathbf{q}})}\frac{\sum_{j,k}\epsilon_{ijk}q_k \operatorname{Re} R_{V_j}^{\Gamma_i}(\mathbf{q};t_{\text{sep}},t)}{\sum_{j\neq i} q_j^2} \tag{7}$$

Q^2-dependence of the isovector form factors on E250

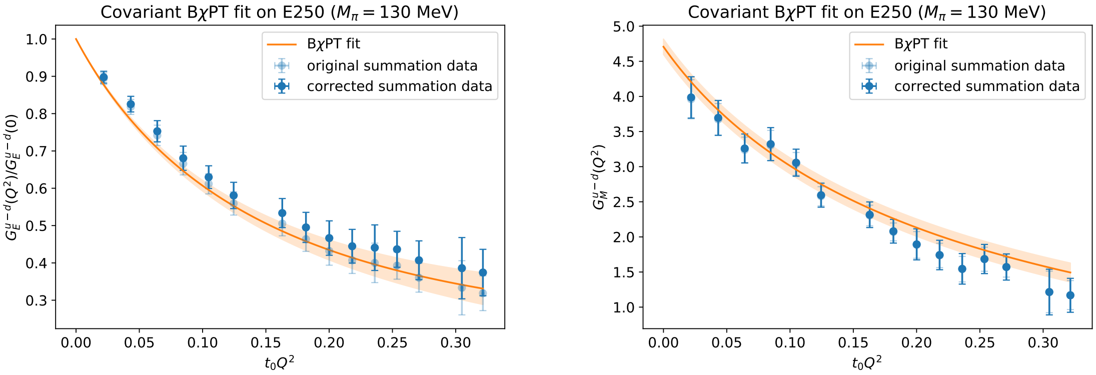

Q^2-dependence of the isoscalar form factors on E250

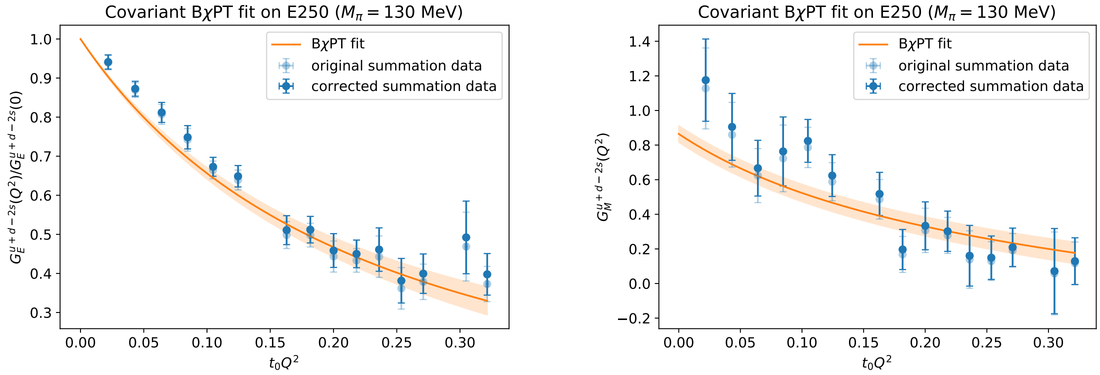

Residuals of the BχPT fits

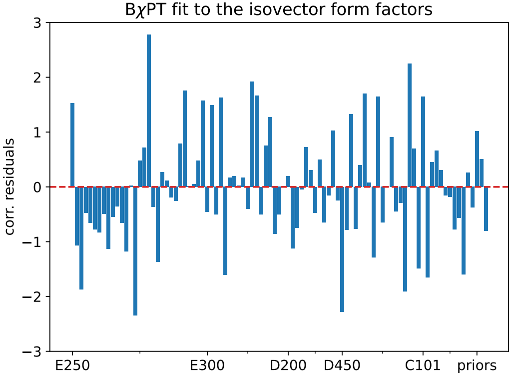

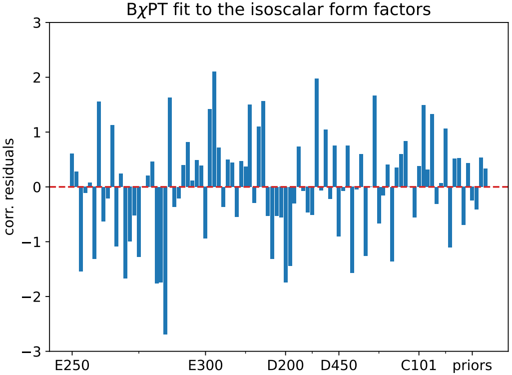

Histograms

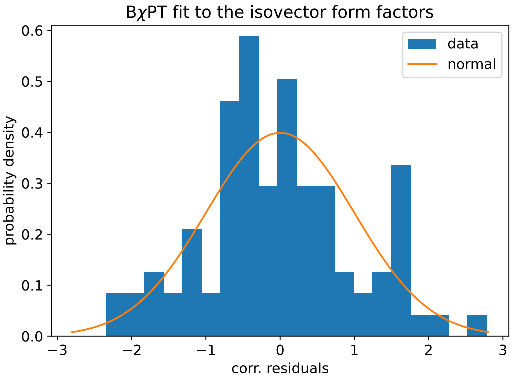
BχPT fit to the isovector form factors
data
normal
probability density
0.0
0.1
0.2
0.3
0.4
0.5
0.6
−3
−2
−1
0
1
2
3
corr. residuals

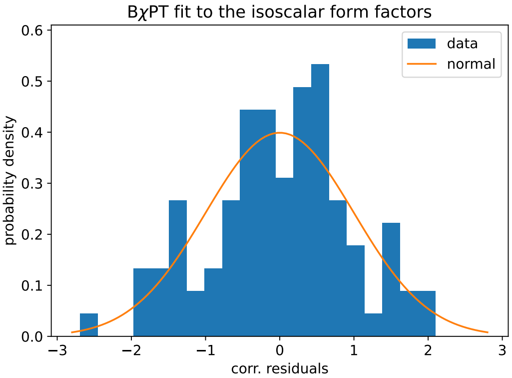
BχPT fit to the isoscalar form factors
data
normal
probability density
0.0
0.1
0.2
0.3
0.4
0.5
0.6
−3
−2
−1
0
1
2
3
corr. residuals

Q-Q plots

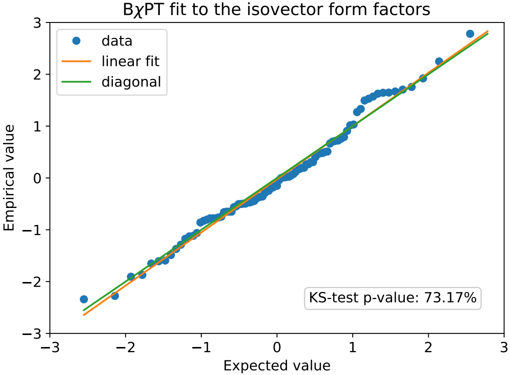
BχPT fit to the isovector form factors
data
linear fit
diagonal
KS-test p-value: 73.17%
Empirical value
Expected value
3
2
1
0
−1
−2
−3

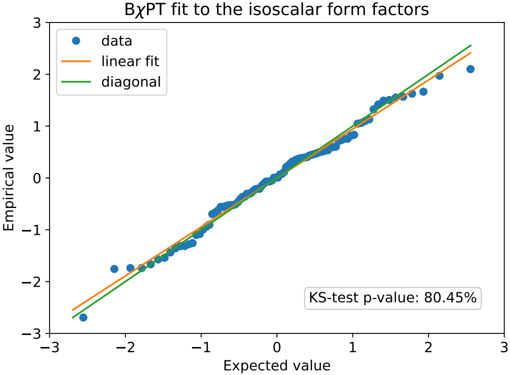
BχPT fit to the isoscalar form factors
data
linear fit
diagonal
KS-test p-value: 80.45%
Empirical value
Expected value
3
2
1
0
−1
−2
−3

Disambiguating the statistical and systematic uncertainties

- Scale the statistical variances of the individual fit results by a factor of $\lambda = 2$
- Repeat the model averaging procedure
- Assumptions:
  - Above rescaling only affects the statistical error of the averaged result
  - Statistical and systematic errors add in quadrature
- Contributions of the statistical and systematic errors to the total error,

$$\sigma^2_{\text{stat}} = \frac{\sigma^2_{\text{scaled}} - \sigma^2_{\text{orig}}}{\lambda - 1}, \qquad \sigma^2_{\text{syst}} = \frac{\lambda\sigma^2_{\text{orig}} - \sigma^2_{\text{scaled}}}{\lambda - 1} \tag{8}$$

- Consistency check: results are almost independent of λ (if it is chosen not too small)

Final results

$$\langle r_E^2\rangle^{u-d} = (0.785 \pm 0.022 \pm 0.026)\ \mathsf{fm}^2$$
$$\langle r_M^2\rangle^{u-d} = (0.663 \pm 0.011 \pm 0.008)\ \mathsf{fm}^2$$
$$\mu_M^{u-d} = 4.62 \pm 0.10 \pm 0.07$$

$$\langle r_E^2\rangle^{u+d-2s} = (0.554 \pm 0.018 \pm 0.013)\ \mathsf{fm}^2$$
$$\langle r_M^2\rangle^{u+d-2s} = (0.657 \pm 0.030 \pm 0.031)\ \mathsf{fm}^2$$
$$\mu_M^{u+d-2s} = 2.47 \pm 0.11 \pm 0.10$$

$$\langle r_E^2\rangle^{p} = (0.672 \pm 0.014 \pm 0.018)\ \mathsf{fm}^2$$
$$\langle r_M^2\rangle^{p} = (0.658 \pm 0.012 \pm 0.008)\ \mathsf{fm}^2$$
$$\mu_M^{p} = 2.739 \pm 0.063 \pm 0.018$$

$$\langle r_E^2\rangle^{n} = (-0.115 \pm 0.013 \pm 0.007)\ \mathsf{fm}^2$$
$$\langle r_M^2\rangle^{n} = (0.667 \pm 0.011 \pm 0.016)\ \mathsf{fm}^2$$
$$\mu_M^{n} = -1.893 \pm 0.039 \pm 0.058$$

- Model-independent description of the Q^2-dependence of the form factors
- Map domain of analyticity of the form factors onto the unit circle,

$$z(Q^2) = \frac{\sqrt{\tau_{\mathrm{cut}} + Q^2} - \sqrt{\tau_{\mathrm{cut}} - \tau_0}}{\sqrt{\tau_{\mathrm{cut}} + Q^2} + \sqrt{\tau_{\mathrm{cut}} - \tau_0}}, \tag{9}$$

  where $\tau_{\mathrm{cut}} = 4M_{\pi,\mathrm{phys}}^2$, and we employ $\tau_0 = 0$
- Expand the form factors as

$$G_E(Q^2) = \sum_{k=0}^{n} a_k z(Q^2)^k, \quad G_M(Q^2) = \sum_{k=0}^{n} b_k z(Q^2)^k \tag{10}$$

- We fix $G_E(0) = a_0 = 1$, use $n = 7$, and incorporate the 4 sum rules for each form factor

Zemach integrand

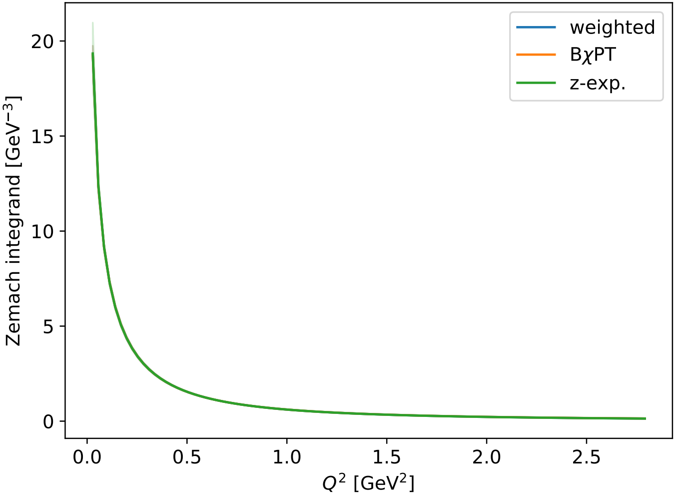

Crosscheck of direct fits with z-expansion: proton magnetic moment

- Use $n = 2$ and no sum rules (focus on low-momentum region)
- Magnetic moment significantly smaller than direct fits, which are compatible with experiment

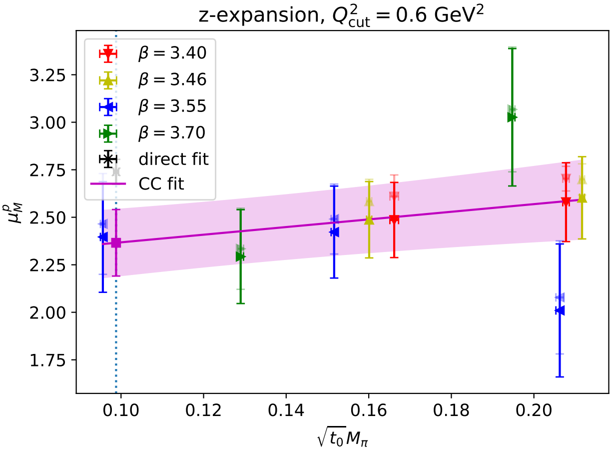

Crosscheck of direct fits with z-expansion: proton electromagnetic radii

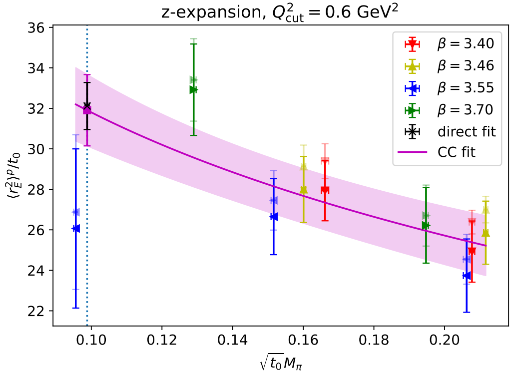

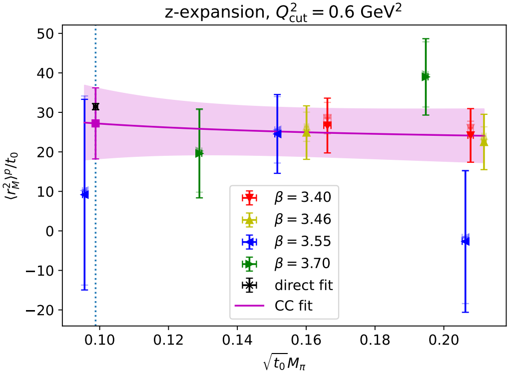

- Radii in good agreement with direct fits, albeit with significantly larger errors
- Not sufficiently stable against fluctuations on single momenta or ensembles